Catalysis Letters 24 (1994) 1–13

Raman investigations of NH_3 adsorption on TiO_2, Nb_2O_5, and Nb_2O_5/TiO_2

Rusty M. Pittman and Alexis T. Bell

Chemical Sciences Division, Lawrence Berkeley Laboratory, Berkeley, CA 94720, USA and Department of Chemical Engineering, University of California, Berkeley, CA 94720-9989, USA

Received 18 August 1993; accepted 11 October 1993

A study has been carried out of the interactions of NH_3 with TiO_2, Nb_2O_5, and Nb_2O_5/TiO_2. Raman spectroscopy was used to characterize the structure of the adsorbed NH_3 and perturbations of species present at the surface of the adsorbent. On each oxide, NH_3 adsorbs predominantly at Lewis acid sites. Hydrogen-bonding occurs between the adsorbed NH_3 and OH groups present on the surface of TiO_2. A small concentration of NH_4^+ is observed, consistent with the relatively low concentration of Brønsted acid sites compared to Lewis acid sites on each of the samples investigated. Exposure of Nb_2O_5/TiO_2 to NH_3 at temperatures up to 500°C does not result in partial reduction of the supported niobia.

Keywords: Ammonia; titania; niobia; titania-supported niobia; Raman spectroscopy

1. Introduction

Catalysts containing niobia dispersed on an oxidic support have been the subject of considerable recent interest. Niobia supported on silica has been shown to be active for the dehydrogenation of ethanol to acetaldehyde [1,2], the dehydration of ethanol to ethene and diethyl ether [2], the photo-oxidation of propene, and the photocatalyzed dehydrogenation of 2-propanol to acetone [3,4]. Titania-supported niobia is active for the selective catalytic reduction (SCR) of NO by NH_3 [5]. While the activity of this catalyst is lower than that of V_2O_5/TiO_2, the addition of a small amount of niobia to V_2O_5/TiO_2 increases the catalyst activity for SCR significantly at lower temperatures [6].

The structure of supported Nb_2O_5 has been characterized by a number of investigators [3,7–18]. These studies indicate that on SiO_2, Al_2O_3, and TiO_2 niobia is present as isolated monomeric and oligomeric species at low Nb loadings but aggregates into a bulk-like structure at higher loadings. A detailed investigation of the structure of Nb_2O_5/TiO_2 has shown that for niobia weight loading above about 2%, the dispersed niobia is present as islands of amorphous Nb_2O_5 [18].

TiO_2 and Nb_2O_5 are known to contain both Brønsted and Lewis acid sites [14]. The present study was undertaken to characterize the interactions of NH_3 with such sites on TiO_2, Nb_2O_5, and Nb_2O_5/TiO_2. The extent to which Nb_2O_5 is reduced by exposure to NH_3 at elevated temperatures was also investigated.

2. Experimental

High surface area (96 m^2/g) anatase was prepared by slow hydrolysis of titanium isopropoxide at 0°C. The resulting product was washed, dried and then calcined in pure O_2 at 400°C for 12 h [18]. Amorphous niobic acid (80% Nb_2O_5 and 20% H_2O) was obtained from Niobium Products company and then calcined at 500°C in pure O_2 for 1 h prior to use. A sample of Nb_2O_5/TiO_2 containing 11.3% by weight of Nb (16.2% by weight of Nb_2O_5) was prepared by incipient wetness impregnation of the high surface area anatase with a hexane solution of niobium ethoxide [18]. Following impregnation, the solid was dried and then calcined at 500°C in pure O_2 for 2 h. The BET surface area of the calcined Nb_2O_5/TiO_2 sample is 91 m^2/g.

Samples for Raman spectroscopy were prepared by pressing a pellet of the powder (10 000 psi). The pellet was placed in a quartz Raman cell [18] which was then purged overnight in flowing He (100 cm^3/min). The sample was then reoxidized in O_2 (100 cm^3/min) for 0.5 h, then cooled down in O_2 to the temperature at which the spectrum was to be collected. During acquisition of a spectrum, the sample was rotated at about 100 rpm to prevent decomposition of the sample due to heating by the laser. Spectra were acquired by using a double monochrometer operated as a spectrophotometer [18]. A single-notch holographic filter (Kaiser Optical HNF-1164) was used to eliminate Rayleigh scattering and the signal was detected by a photodiode array (Princeton Instruments EIRY 1000).

The gases used in this study include: helium (Alphagaz, 99.9999%); hydrogen (Amerigas, 99.999%); oxygen (Alphagaz, 99.997%); and 1.1% NH_3/He (Matheson). With the exception of the NH_3/He mixture, each of the gases was passed through a molecular sieve bed to remove traces of water.

3. Results and discussion

3.1. ADSORPTION OF NH_3 ON TiO_2

Fig. 1 displays Raman spectra in the region of 3000–4000 cm^{-1} taken before and after NH_3 adsorption on TiO_2. Spectrum a shows O–H stretching peaks for TiO_2 taken at room temperature following calcination in flowing O_2 (100 cm^3/min) at 500°C for 0.5 h. A strong peak is observed at 3718 cm^{-1} together with a series of weaker, overlapping peaks at 3635, 3667, and 3682 cm^{-1}. Spectrum b was

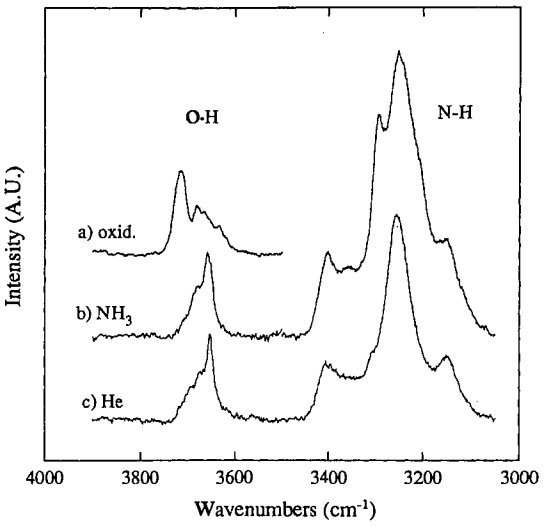

Fig. 1. Spectra of the O–H and N–H stretching regions for TiO_2: (a) following calcination at 500°C; (b) after exposure to 1.1% NH_3/He for 0.5 h; (c) after purging overnight in He. All spectra recorded at room temperature.

taken following exposure of the sample to a mixture of 1.1% NH_3/He (100 cm^3/min) for 0.5 h at room temperature. NH_3 adsorption results in the attenuation of the OH peak at 3718 cm^{-1} and the appearance of a new OH peak at 3660 cm^{-1}, as well as the appearance of six peaks attributable to N–H stretching vibrations located at 3148, 3206, 3250, 3295, 3361, and 3404 cm^{-1}. A spectrum of H–N–H bending vibrations for adsorbed NH_3 is presented in fig. 2. Following NH_3 adsorption, bands are observed at 1220, 1440, 1600, and 1670 cm^{-1}. Spectrum c in fig. 1 was recorded following a purge of the Raman cell with flowing He (100 cm^3/min) overnight. Purging has virtually no effect on the OH peaks, but results in a significant loss in intensity of the sharp peak at 3295 cm^{-1} and the weak shoulder at 3206 cm^{-1}, as well as a partial loss in intensity of the bands located at 3148, 3250, and 3404 cm^{-1}.

The positions of the hydroxyl peaks observed in the spectrum of calcined anatase, shown in fig. 1, are very similar to those reported by Busca et al. [19]. The observed bands can be attributed to Ti–OH groups affected by varying degrees of hydrogen bonding or interaction of the hydroxyl oxygen atom with adjacent titanium cations. The loss in intensity in the peak at 3718 cm^{-1} and the corresponding appearance of a band at 3660 cm^{-1} is ascribed to perturbation of the hydroxyl vibrations by hydrogen bonding to NH_3, in a manner similar to that reported for NH_3 adsorbed on SiO_2 [20,21].

The NH peaks observed in figs. 1 and 2 can be assigned on the basis of previous studies [19,22–26]. The peaks at 3148, 3250, and 3404 cm^{-1} are due to the $2\nu_4$, ν_1,

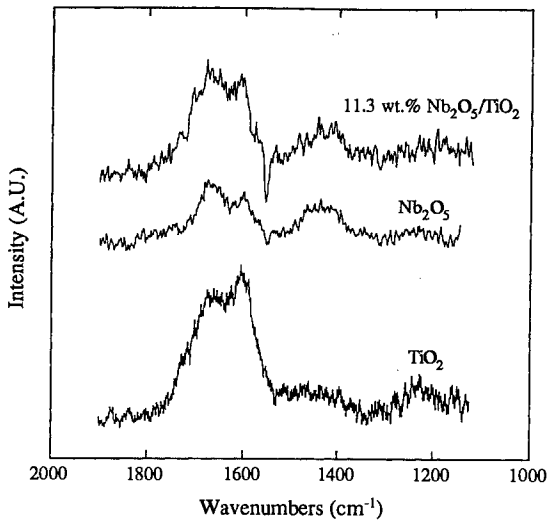

Fig. 2. Spectra of the H–N–H bending region obtained for NH_3 adsorbed on TiO_2, niobic acid, and 11.3 wt% Nb/TiO_2. In each case, the spectrum of calcined TiO_2 has been subtracted from the spectrum of NH_3 adsorbed on the sample. All spectra recorded at room temperature.

and ν_3 stretching modes of NH_3 strongly adsorbed on Ti^{4+} Lewis acid sites, whereas the peaks at 3206 and 3295 cm^{-1} are due to the $2\nu_4$ and ν_1 stretching modes of weakly adsorbed NH_3. The weak NH peak at 3361 cm^{-1} is attributable to NH_x ($x = 1, 2$) species formed by the decomposition of NH_3. The peaks appearing at 1600 and 1220 cm^{-1} in fig. 2 are assigned to the asymmetric and symmetric bending modes of adsorbed NH_3, whereas the peaks appearing at 1670 and 1440 cm^{-1} are assigned to the same modes for adsorbed NH_4^+ [19,23,27].

The relative amounts of adsorbed NH_3 and NH_4^+ are difficult to ascertain from the spectra presented in figs. 1 and 2. However, the relative concentrations of these species can be inferred from measurements of the concentrations of Lewis and Brønsted acid sites on anatase. Studies on different anatase samples show that Brønsted acidity is only observed for samples with surface areas in excess of 120 m^2/g [28]. Consistent with this, measurements of pyridine adsorption on a sample of Degussa P-25 TiO_2 (90% anatase and 10% rutile) having a BET surface area of 50 m^2/g shows only Lewis acid sites and no evidence for Brønsted acid sites [15]. These observations suggest that the anatase sample used in the present study should have very few Brønsted sites and, hence, that most of the adsorbed NH_3 is attached to Lewis acid sites.

The distinctions between weakly and strongly adsorbed NH_3 can be understood from a recent ^2H NMR study of NH_3 adsorbed on rutile [29]. For coverages below 0.7 of a monolayer, the ^2H spectrum is a powder pattern characteristic of NH_3 adsorbed on Lewis acid sites, freely rotating around the Ti–N bond axis. Above an NH_3 coverage of 0.7, the ^2H spectrum is dominated by a singlet, indicating rapid

sampling of molecular orientations such that the time average of the quadrupolar energy is zero. The change in shape of the ^2H NMR spectrum of NH_3 at high coverages is ascribed to repulsive lateral interactions which cause a weakening in the strength of NH_3 adsorption and, hence, an increase in the rotational mobility of the adsorbed molecules. These results suggest that the reduction in the strength of NH_3 adsorption at high coverage observed in the present study may be due to repulsive lateral interactions.

3.2. ADSORPTION OF NH_3 ON Nb_2O_5

Spectrum a in fig. 3 shows Raman spectra of NH_3 adsorbed at room temperature on bulk niobic acid that has been calcined in flowing O_2 at 500°C for 1 h. Six N–H stretching peaks located at 3161, 3218, 3261, 3299, 3360, and 3400 cm^{-1} are evident in the spectrum recorded during the passage of a 1.1% NH_3/He mixture over the sample at room temperature. The corresponding H–N–H bending bands are presented in fig. 2. Four bands are observed at 1220, 1400, 1600, and 1670 cm^{-1}. When the Raman cell is purged with flowing He overnight, all of the N–H stretching peaks seen in fig. 3 are attenuated significantly (see spectrum b), particularly the strong feature appearing at 3299 cm^{-1} and the weak shoulder at 3218 cm^{-1}.

The positions of the peaks for NH_3 adsorbed on calcined Nb_2O_5 are very similar to those observed on TiO_2, and, hence these features can be assigned by analogy with those proposed for TiO_2. Comparison of the spectra presented in figs. 1 and 3

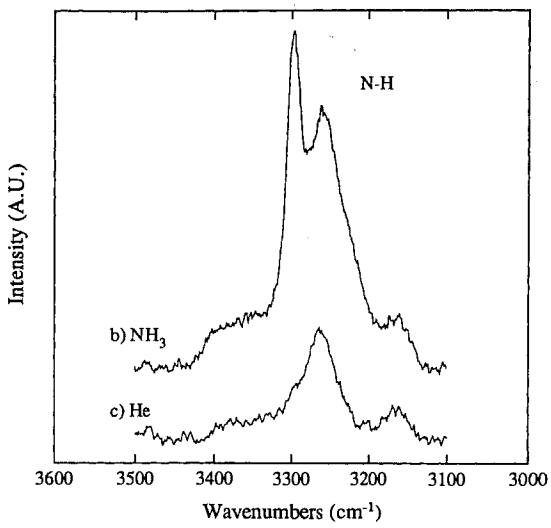

Fig. 3. Spectra of the N–H stretching region for NH_3 adsorbed on niobic acid: (b) after exposure to 1.1% NH_3/He for 0.5 h; (c) after purging overnight in He. All spectra recorded at room temperature.

shows that under identical adsorption conditions the ratio of weakly to strongly adsorbed NH_3 is greater for Nb_2O_5 than TiO_2. It is also evident that the strongly adsorbed NH_3 is more weakly bound on Nb_2O_5 than TiO_2, as can be judged by the extent of loss in NH peak intensities upon purging in He. These observations indicate that NH_3 is adsorbed more weakly on Nb_2O_5 than on TiO_2. In agreement with this, the frequency of the ν_1 vibrational mode of NH_3 is higher for Nb_2O_5 ($\nu_1 = 3261\,cm^{-1}$) than for TiO_2 ($\nu_1 = 3250\,cm^{-1}$).

In contrast to TiO_2, the adsorption of NH_3 does alter the spectrum of the Nb_2O_5. As seen in fig. 4, the spectrum of calcined Nb_2O_5 consists of broad bands at 660 and 890 cm^{-1}, and weaker peaks at 940 and 995 cm^{-1}. The bands at 660 and 890 cm^{-1} are attributable to Nb–O–Nb stretching vibrations in amorphous Nb_2O_5, whereas the peaks at 940 and 995 cm^{-1} are due to Nb=O vibrations present at the surface of the oxide [14–18]. Adsorption of NH_3 results in the disappearance of the bands at 940 and 995 cm^{-1}, but has no other effect on the spectrum of Nb_2O_5. Purging of the sample in He has no effect on the spectrum. The broadening of the band at 660 cm^{-1} is an artifact caused by the onset of detector saturation in the region between 600 and 700 cm^{-1}. The loss in intensity of the peaks at 940 and 995 cm^{-1} upon adsorption of NH_3 is identical to that observed when Nb_2O_5 is exposed to H_2O, and can be ascribed to the formation of Lewis acid–base adducts between the lone pair of electrons on the nitrogen atom of NH_3 and Nb^{5+} cations in Nb=O groups. It is envisioned that the interaction with NH_3 weakens the Nb=O bond causing a downscale shift in its frequency, or, possibly, the formation of $Nb(OH)(NH_2)$ groups. This latter reaction might explain the presence of the NH_2 band observed at 3360 cm^{-1}.

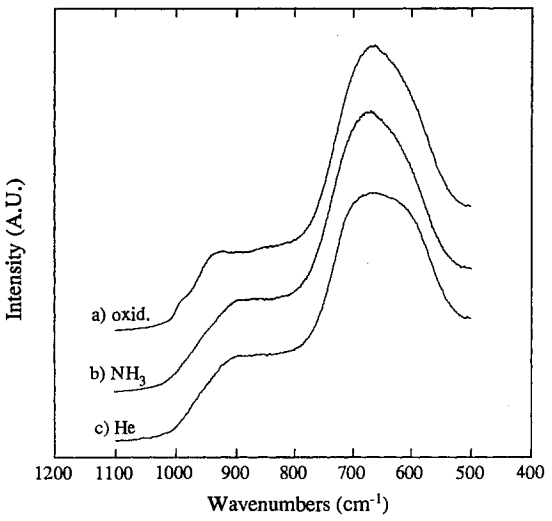

Fig. 4. Spectra of the Nb–O stretching region for niobic acid: (a) after calcination at 500°C; (b) after exposure to 1.1% NH_3/He for 0.5 h; (c) after purging overnight in He.

3.3. ADSORPTION OF NH_3 ON Nb_2O_5/TiO_2

Spectra showing the effects of NH_3 adsorption on Nb_2O_5/TiO_2 are presented in fig. 2 and figs. 5–7. The OH spectrum of a calcined sample of Nb_2O_5/TiO_2 is similar to that of pure anatase except that the principal feature at 3718 cm^{-1} is only one-quarter as intense [18]. From this it can be inferred that the dispersed niobia covers roughly 75% of the titania surface. This is not unreasonable since the loading of niobia in the 11.3% Nb sample corresponds to 1.45 theoretical monolayers of titania. Adsorption of NH_3 causes a loss of intensity in the peak at 3718 cm^{-1}. Purging of the NH_3-exposed sample in He at room temperature has no effect on the OH spectrum, but heating in He to temperatures of 100°C and above results in a complete loss of all OH features.

Fig. 6 shows spectra for the N–H stretching vibrations of NH_3 adsorbed on Nb_2O_5/TiO_2, whereas fig. 2 shows a spectrum for H–N–H bending vibrations. Upon initial dosing with NH_3 bands appear at 3151, 3252, and 3405 cm^{-1}, as can be seen in fig. 6. Further exposure to NH_3 produces additional features at 3207,

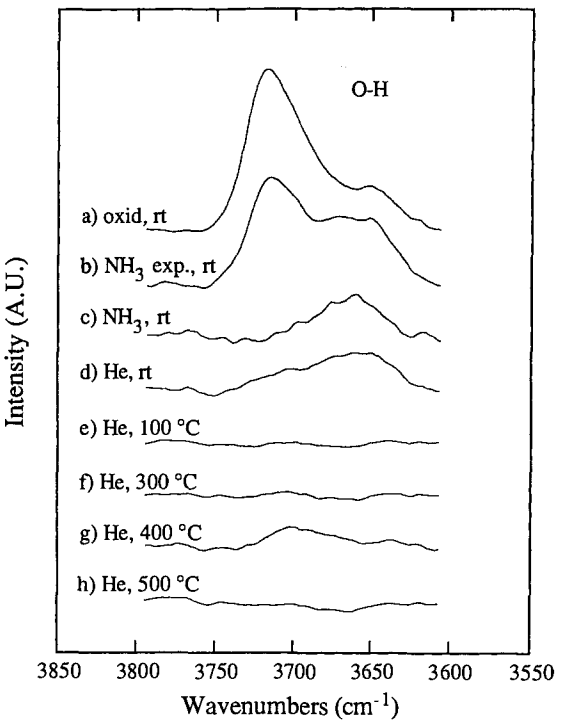

Fig. 5. Spectra of the O–H stretching region of 11.3 wt% Nb/TiO_2 taken after NH_3 adsorption at room temperature and subsequent purging in He at elevated temperatures: (a) after calcination at 500°C; (b) after exposure to a small dose of NH_3; (c) after continuous exposure to 1.1% NH_3/He for 0.5 h; (d) after purging in He at room temperature; (e–h) after purging in He at progressively higher temperatures.

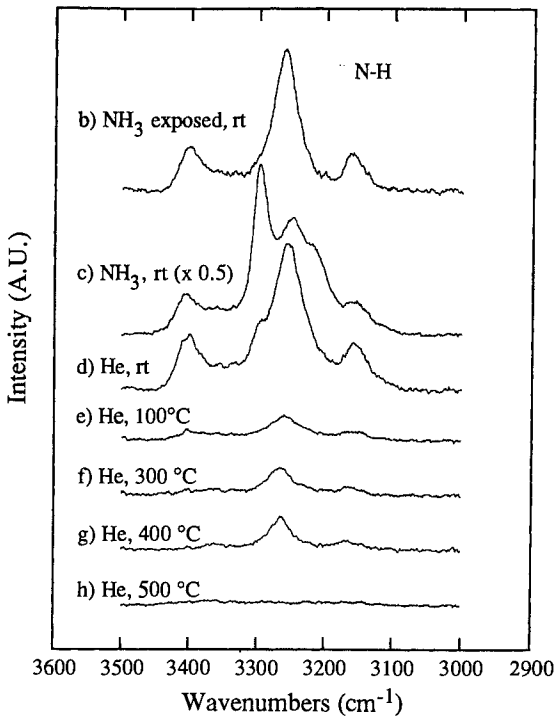

Fig. 6. Spectra of the N–H stretching region of 11.3 wt% Nb/TiO_2 taken after NH_3 adsorption at room temperature and subsequent purging in He at elevated temperatures: (b) after exposure to a small dose of NH_3; (c) after continuous exposure to 1.1% NH_3/He for 0.5 h; (d) after purging in He at room temperature; (e–h) after purging in He at progressively higher temperatures.

3298, and 3365 cm^{-1}. Purging in He overnight at room temperature reduces the intensities of the bands at 3207 and 3298 cm^{-1} very significantly. Additional desorption of NH_3 occurs when the sample is heated in flowing He at temperatures between 100 and 400°C. Bending vibrations for strongly adsorbed NH_3 are seen in fig. 2 at 1220, 1440, 1600, and 1670 cm^{-1}.

The positions of the stretching and bending vibrations of NH_3 adsorbed on Nb_2O_5/TiO_2 are quite similar to those observed for NH_3 adsorbed on TiO_2 and Nb_2O_5 and, hence, the interpretation of these features is the same. Thus, the bands at 3151, 3252, and 3405 cm^{-1} are assigned to stretching vibrations of strongly adsorbed NH_3, whereas the bands at 3207 and 3298 cm^{-1} are assigned to similar vibrations for weakly adsorbed NH_3. The bands at 1220 and 1600 cm^{-1} are assigned to bending vibrations of adsorbed NH_3, whereas the bands at 1440 and 1670 cm^{-1} are assigned to bending vibrations in adsorbed NH_4^+. The weak band at 3365 cm^{-1} is attributed to stretching vibrations of adsorbed NH_x ($x = 1, 2$) species. The strong intensity of the peak at 3298 cm^{-1} relative to the other N–H stretching peaks is only observed for niobic acid, suggesting that most of the weakly bound NH_3 is present on the dispersed niobia.

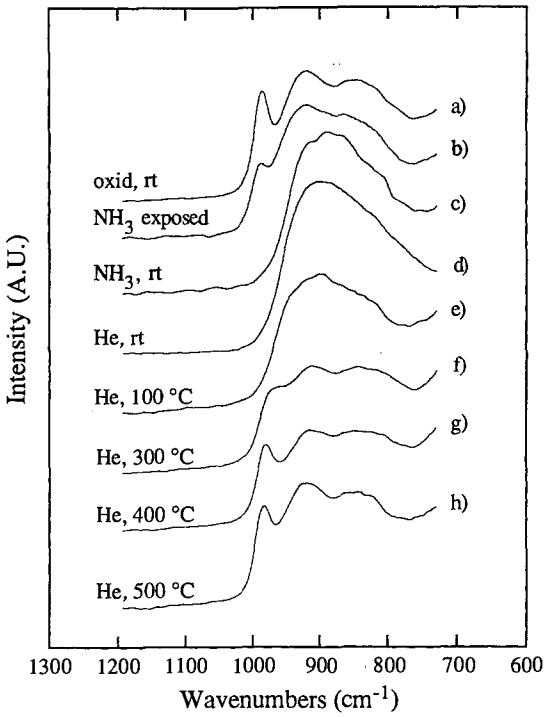

Fig. 7. Spectra of the Nb–O stretching region of 11.3 wt% Nb/TiO_2 after NH_3 adsorption at room temperature and subsequent purging in He at elevated temperatures: (a) after calcination at 500°C; (b) after exposure to a small dose of NH_3; (c) after continuous exposure to 1.1% NH_3/He for 0.5 h; (d) after purging in He at room temperature; (e–h) after purging in He at progressively higher temperatures.

Comparison of the spectra in fig. 6 with those in figs. 1 and 3 suggests that the strength of NH_3 adsorption and the proportion of weakly versus strongly bound NH_3 are intermediate between those observed for TiO_2 and Nb_2O_5. In the discussion of the OH bands observed on Nb_2O_5/TiO_2 presented above, it was estimated that 75% of the surface of TiO_2 is covered by dispersed niobia. If this is correct, then comparison of the NH_3 spectra presented in figs. 1, 3, and 6 suggests that a significant fraction of the NH_3 adsorbed on Nb_2O_5/TiO_2 occurs on the support.

The relative intensities of the bands for the bending vibrations of NH_3 and NH_4^+, shown in fig. 2, suggest that the concentration of the latter species is somewhat greater on Nb_2O_5/TiO_2 than on TiO_2, similar to what is observed for bulk Nb_2O_5. This trend is consistent with the higher Brønsted acidity of Nb_2O_5 and Nb_2O_5/TiO_2 relative to TiO_2 [15,30]. It is noted, though, that even at a loading of 10 wt% Nb_2O_5 on TiO_2 (50 m^2/g) the ratio of Brønsted to Lewis acid sites is only 0.06 [15].

The influence of adsorbed NH_3 on the spectrum of niobia is shown in fig. 7. The spectrum of pure titania was subtracted from that of Nb_2O_5/TiO_2, to permit

observation of features in the region of 500–800 cm^{-1}. NH_3 adsorption causes a decrease in the intensity of the peaks at 940 and 995 cm^{-1} associated with the stretching vibrations of Nb=O groups present at the surface of small islands of dispersed amorphous niobia. A corresponding increase in intensity can be observed in the vicinity of 900 cm^{-1}. These changes are similar to those observed in fig. 4 for bulk Nb_2O_5. It is proposed that the growth in intensity in the region near 900 cm^{-1} is attributable to vibrations of Nb=O bonds associated with Nb=O groups participating in Lewis acid–base adducts with NH_3. Purging the sample in He at room temperature causes little change in the spectrum, but upon raising the temperature to 100°C, a noticeable loss of intensity in the region near 900 cm^{-1} and a slight increase in the intensity of the spectrum above 950 cm^{-1} occur. Further increasing the temperature restores the appearance of the spectrum to that observed following calcination of the sample prior to NH_3 adsorption.

The effects of NH_3 exposure at elevated temperatures are presented in figs. 8 and 9. Fig. 8 shows that with increasing adsorption temperature, the proportion of weakly adsorbed NH_3 (ν_{NH} = 3206, 3295 cm^{-1}) rapidly decreases, whereas the intensity of the bands for strongly adsorbed NH_3 (ν_{NH} = 3148, 3250, 3404 cm^{-1}) pass through a maximum near 400°C. The increase in the intensity of the peaks for

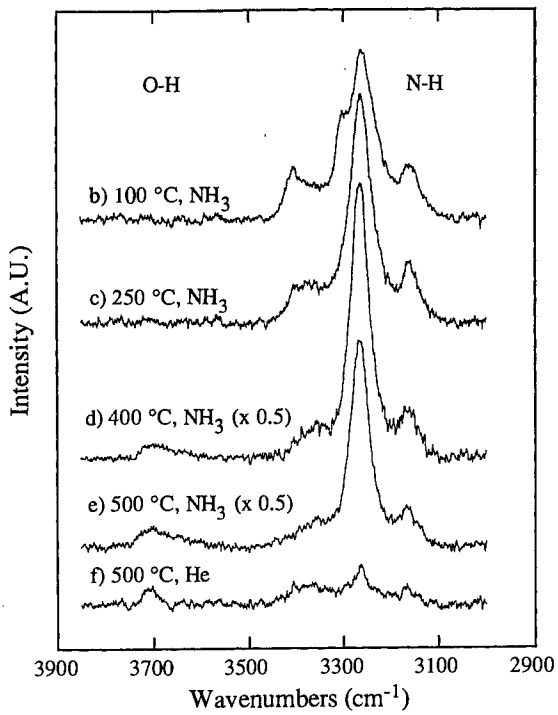

Fig. 8. Spectra of the N–H stretching region taken after exposure of 11.3 wt% Nb/TiO_2 to NH_3 at progressively higher temperatures (b–e); (f) after purging in He at 500°C. Spectra (e) and (f) have been multiplied by a factor of 0.5.

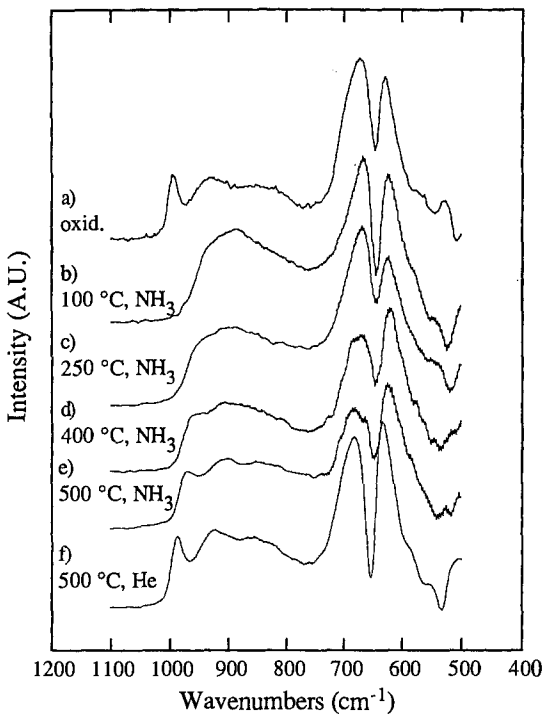

Fig. 9. Spectra of the Nb–O stretching region of 11.3% Nb/TiO_2 taken after NH_3 exposure at various temperatures: (a) after calcination at 500°C; (b–e) after exposure to NH_3 at progressively higher temperatures; (f) after purging in He at 500°C.

strongly adsorbed NH_3 occurring between 100 and 400°C may be due to the progressive displacement of adsorbed water formed by partial decomposition of adsorbed NH_3. This interpretation is supported by studies showing that H_2O will displace NH_3 adsorbed on rutile [31].

Fig. 9 illustrates the changes in the spectrum of dispersed niobia caused by the exposure of the sample to NH_3 at elevated temperatures. As in the case of the spectra presented in fig. 7, the spectra shown in fig. 9 have had the spectrum of pure titania subtracted from that of Nb_2O_5/TiO_2, to permit observation of features in the region between 500 and 800 cm^{-1}. The negative peak appearing in the center of the Nb–O–Nb peak at 660 cm^{-1} is due to titania and arises from the subtraction of a titania spectrum in which this feature is somewhat more intense than in the spectrum of Nb_2O_5/TiO_2. The only changes observed in the spectrum upon adsorption of NH_3 at elevated temperatures are those occurring in the region above 900 cm^{-1}. As in fig. 7, the presence of NH_3 causes a loss of intensity in the Nb=O peaks at 940 and 995 cm^{-1} and an increase in the intensity of the spectrum near 900 cm^{-1}. For temperatures above 400°C, the effects of NH_3 adsorption are reversed, though, reflecting progressively less interaction of NH_3 with the sample.

It is important to note that even at 500°C, no evidence is seen in fig. 9 for the reduction of the dispersed niobia, as might be indicated by a permanent loss in intensity of features associated with either Nb=O of Nb–O–Nb vibrations. This observation contrasts strongly with what has been reported recently for the interactions of NH_3 with V_2O_5/TiO_2 [32]. For dispersed vanadia, exposure to NH_3 at elevated temperatures results in a partial reduction of the dispersed oxide. Further indication of the stability of dispersed niobia to reduction was obtained by exposing the 11.3% Nb sample to 1 atm of flowing H_2 at 500°C for 1 h. After purging the sample in He at 500°C for 0.5 h to desorb any adsorbed water vapor, the spectrum of the sample was identical to that observed after calcination (see fig. 9). These observations are consistent with the fact that the change in the standard free energy at 500°C for reduction of Nb_2O_5 to NbO_2 is 7.1 kcal/mol of H_2 consumed, whereas the standard free energy change for the reduction of V_2O_5 to VO_2 is −34.1 kcal/mol of H_2 consumed. The higher stability of niobium oxide in a high oxidation than the corresponding vanadium oxide is characteristic of second-row compared to first-row transition metals [33].

4. Conclusions

Ammonia adsorption on TiO_2, Nb_2O_5, and Nb_2O_5/TiO_2 occurs predominantly on Lewis acid sites. The adsorbed NH_3 is present in two forms corresponding to weak and strong adsorption. Strong adsorption occurs at low NH_3 coverages and is attributed to specific Lewis acid–base adducts formed between NH_3 and Ti^{4+} or Nb^{5+} cations. A weakening in the strength of NH_3 adsorption occurs at high coverages due to repulsive lateral interactions between adjacent NH_3 molecules. Evidence is seen, as well, for hydrogen-bonding of adsorbed NH_3 with hydroxyl groups present on the surface of titania. The relative strength of NH_3 adsorption on titania is greater than on either bulk or dispersed niobia. A small amount of NH_4^+ is observed in addition to adsorbed NH_3. This species is formed by the interaction of NH_3 with Brønsted acid sites on the adsorbent. The presence of only a small amount of NH_4^+ is attributed to the low concentration of Brønsted acid sites on each of the samples studied. Exposure of Nb_2O_5/TiO_2 to NH_3 at temperatures up to 500°C does not reduce the dispersed niobia, in contrast to what is observed for titania-supported vanadia. This observation is consistent with the higher thermodynamic stability of niobia relative to vanadia.

Acknowledgement

This work was supported by the Director, Office of Energy Research, Office of Basic Energy Sciences, Chemical Sciences Division of the US Department of Energy under Contract No. DE-AC03-76-SF00098.

References

[1] M. Nishimura, K. Asakura and Y. Iwasawa, J. Chem. Soc. Chem. Commun. (1986) 1660.
[2] M. Shirai, N. Ichikuni, K. Asakura and Y. Iwasawa, Catal. Today 8 (1990) 57.
[3] S. Yoshida, Y. Nishimura, T. Tanaka, H. Kanai and T. Funabiki, Catal. Today 8 (1990) 67.
[4] Y. Wada and A. Morikawa, Bull. Chem. Soc. Japan 60 (1987) 3509.
[5] S. Okazaki and T. Okuyama, Bull. Chem. Soc. Japan 56 (1983) 2159.
[6] K. Tanabe, Catal. Today 8 (1990) 1.
[7] S. Yoshida, T. Tanaka, T. Hanada, H. Hiraiwa, H. Kanai and T. Funabiki, Catal. Lett. 12 (1992) 227.
[8] T. Tanaka, H. Nojima, H. Yoshida, H. Nakagawa, T. Funabiki and S. Yoshida, Catal. Today 16 (1993) 297.
[9] P.A. Burke and E.I. Ko, J. Catal. 129 (1991) 38.
[10] E.I. Ko, R. Bafrali, N.T. Nuhfer and N.J. Wagner, J. Catal. 95 (1985) 260.
[11] J.G. Weissman, E.I. Ko and P. Wynblatt, J. Catal. 108 (1987) 383.
[12] K. Asakura and Y. Iwasawa, Chem. Lett. (1986) 859.
[13] N. Ichikuni and Y. Iwasawa, Catal. Today 16 (1993) 427.
[14] I.E. Wachs, J.-M. Jehng, and F.D. Hardcastle, Solid State Ionics 32/33 (1989) 904.
[15] J.-M. Jehng and I.E. Wachs, Catal. Today 8 (1990) 37.
[16] J.-M. Jehng and I.E. Wachs, J. Mol. Catal. 67 (1991) 369.
[17] J.-M. Jehng and I.E. Wachs, J. Phys. Chem. 95 (1991) 7373.
[18] R.M. Pittman and A.T. Bell, J. Phys. Chem., in press.
[19] G. Busca, H. Saussey, O. Saur, J.C. LaValley and V. Lorenzelli, Appl. Catal. 14 (1985) 245.
[20] N.W. Cant and L.H. Little, Can. J. Chem. 42 (1964) 802.
[21] R.A. Rajadhyaksha and H. Knözinger, Appl. Catal. 51 (1989) 81.
[22] M. Primet, P. Pichat and M. Mathieu, J. Phys. Chem. 75 (1971) 1221.
[23] N. Topsøe, J. Catal. 128 (1991) 499.
[24] G. Ramis, G. Busca, V. Lorenzelli and P. Forzatti, Appl. Catal. 64 (1990) 243.
[25] A.A. Tsyganenko, D.V. Posdnyakov and V.N. Filimonov, J. Mol. Struct. 29 (1975) 299.
[26] G.T. Went and A.T. Bell, Catal. Lett. 11 (1991) 111.
[27] K. Nakamoto, *Infrared and Raman Spectra of Inorganic and Coordination Compounds*, 4th Ed. (Wiley, New York, 1977) p. 167.
[28] K. Morishige, F. Kanno, S. Ogawara and S. Sasaki, J. Phys. Chem. 89 (1985) 4404.
[29] B. Boddenberg and R. Niepmann, Mol. Phys. 79 (1993) 405.
[30] K. Tanabe, *Solid Acid and Bases* (Academic Press, New York, 1970).
[31] G.D. Parfitt, J. Ramsbotham and C.H. Rochester, Trans. Faraday Soc. 67 (1971) 841.
[32] G.T. Went, L.-J. Leu and A.T. Bell, J. Catal. 134 (1992) 479.
[33] J.D. Hill, I.G. Worsley and L.G. Hepler, Chem. Rev. 71 (1971) 127.